Hardfacing Characteristics of S42000 Stainless Steel by Using CO_2 Laser

Chien-Kuo Sha and Hsien-Lung Tsai

(Submitted 12 June 2000; in revised form 24 October 2000)

Continuous wave carbon-dioxide (CW CO_2) laser was employed to study the hardfacing characteristics of cladding S42000 stainless steel powder on K02600 mild steel. The cladding layer was overlapped track-by-track and then layer-by-layer. Identical hardfacing on mild steel by submerged arc welding (SAW) was also studied. The wear test, microhardness test, metallographic analysis, scanning electron microscope (SEM) analysis, and electron probe microanalysis (EPMA) were subsequently carried out to compare these hardfacing techniques. The results showed that the hardness of laser cladding was twice the hardness of SAW cladding, and the results indicated that the former had superior wear properties to the latter.

Keywords CO_2 laser, hardfacing, S42000 stainless steel, scanning electron microscope, submerged arc welding, wear mechanisms

1. Introduction

Hardface cladding, mainly by SAW, has been adopted in the area of reclamation for many years.[1–4] Recently, the laser manufacturing technique has expanded its applications to the field of material surface treatment due to its high energy density $10^5 \cdot 10^7$ W cm^2,[5–8] which can locally heat and instantly melt a metal surface as well as provide rapid quenching. High energy density can lower the dilution, narrow the heat-affected zone, reduce thermal distortion, and give a finer microstructure, which in turn improve the coating properties.[6,9–11] Such characteristics expand the utilities of materials, especially on the occasions where resistance to wear and corrosion are essential.[12–15]

The local heating characteristic of the laser can only produce a thin cladding layer. To reach a large area of thick cladding layer, a multicladding technique must be conducted. This can be accomplished by overlapping the tracks with a fixed distance track-by-track, and then layer-by-layer. Some efforts have been made for the overlapping of the laser cladding process.[10,16,17]

To date, because of its high deposition rate, the reclamation of shell mill rolls is traditionally produced by SAW. Due to its high thermal stress, preheat and subsequent tempering is necessary for SAW cladding to avoid cracking.[1,2,3] However, hardness drops after tempering will deteriorate wear resistance.[12] In contrast, there is little thermal stress on the surface of the cladding produced by laser, rendering the preheat and postheat treatment unnecessary. Such advantages promote laser cladding to replace SAW in local area reclamation.

The present research evaluates the differences between the two methods of hardfacing, in regard to the microstructure and hardness distribution. Wear behavior of the cladding layers produced by both methods was also investigated.

Chien-Kuo Sha and **Hsien-Lung Tsai,** Department of Mechanical Engineering, National Taiwan University of Science and Technology, Taipei, Taiwan 106, China. Contact e-mail: D8303501@mail.ntust.edu.tw.

2. Experimental Procedures

In this study, both laser cladding and SAW techniques were carried out using identical cladding materials on low carbon steels. Chemical compositions of the cladding materials and substrates for both methods are shown in Table 1. Primary parameters for both methods are listed in Table 2.

The power source of Rofin Sinar 820 (San Jose, CA) was used for laser cladding, which was conducted with 1.2 kW CW CO_2 laser in the TEM_{00} (transverse electromagnetic mode) pattern. Plates of K02600 steel measuring 100 × 50 × 20

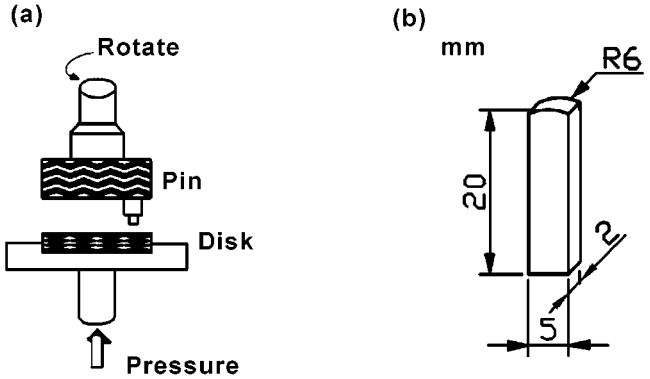

Fig. 1 Wear test: (**a**) pin on disk tester and (**b**) pin specimen size

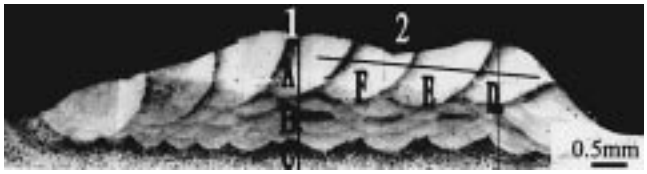

Fig. 2 Cross-sectional microstructure of the multicladding layer produced by laser cladding

Table 1 Chemical compositions of coating materials and substrates for hardfacing

Material UNS		Chemical compositions (wt.%)						
		C	Si	Mn	S	P	Ni	Cr
Filler material	S42000 powder	0.26–0.4	1.00	1.00	0.03	0.04	…	12–14
	Lincoln S42000 wire	0.44	0.40	1.65	0.01	0.02	0.09	15.20
Substrate	K02600	0.15	0.34	1.06	0.01	0.02	0.02	0.06

Table 2 Parameters for hardfacing

Laser		Submerged arc	
Laser power (W)	1200	Welding current (A, ampere)	550
Powder feed rate (g/min)	13.3	Welding voltage (V)	30
Focus length (mm)	190.5	Welding speed (cm/min)	30
Defocus distance (mm)	4.5	Electrode extension distance (mm)	19
Spot size (mm)	3	Flux	Lincoln weld 801
Cladding speed (mm/sec)	10	Preheat temperature (°C)	209
Shroud gas (Argon) flow rate (1/min)	0.5	Postheat temperature (°C)	600
Overlap	50%	Overlap	50%
Cladding tracks per layer	8	Cladding tracks per layer	4
Cladding layers	8	Cladding layers	4

mm were selected as the experimental substrates. The cladding powder UNS S42000 was introduced to the molten pool with argon carrier gas from a coaxial powder feeder. A time of 20 min was allowed for cooling between the successive layers.

The power source of Lincoln DC-1500NA-3N was used for SAW. A low carbon steel K02600 with dimensions 300 × 100 × 25 mm was used as the substrate. The cladding material was Lincoln S42000 (Cleveland, OH) martensitic stainless steel flux core wire with the diameter of ϕ 3.2 mm. Lincoln weld 801 flux was used. The substrates were preheated at 210 °C for 1 h, while the wire and flux were preheated at 250 °C for 3 h. The specimens were tempered at 600 °C for 1 h after cladding.

An Optical microscope and a scanning electron microscope (SEM) were used to study the microstructures in different zones of the cladding layer. The composition distribution was determined using a glow discharge optic emission spectrometer (GD-OES 7500), energy dispersive x-ray (EDX), and electron probe microanalysis (EPMA). A Leitz Minilod (Germany) microhardness tester with a load of 1.961 N was used to investigate the hardness distribution at different locations.

Wear tests were performed on a pin-on-disk type continuous sliding tester with a load of 5 kg, as shown on Fig. 1(a). The sliding distance was 5000 m, with speeds 0.25, 0.5, 0.75, 1, and 1.25 m/s. The disk material was AISI 52100 bearing steel with hardness HRc 61.2. The dimensions of the pin, 20 × 5 × 2 mm, with a radius of 6 mm at one end, are shown on Fig. 1(b). The removed volume of the pin determined the wear loss. The worn surfaces and the debris morphologies were characterized using an SEM.

3. Experimental Results and Discussion

3.1 Microstructural Features of Laser Claddings

Laser cladding is a rapid heating and solidifying process. The microstructures of the cladding layer vary substantially under different process parameters. The temperature gradient (G) of 10^5 °C/cm can be reached, and the growth rate (R) of cm/s approaches the cladding speed. Meanwhile, the cooling rate (GR) of $10^4 \sim 10^8$ °C/s can be attained, depending on the processing parameters.[18,19] The constitutional supercooling (G/R) governs the mode of solidification. The greater degree of constitutional supercooling induces the greater tendency for a given material to switch from the cellular to the dendritic mode of solidification. On the other hand, the cooling rate (GR) governs the scale of the solidification structure; the greater cooling rate produces the finer structure.[20]

A cross section of multicladding layers (8 layers × 8 tracks) microstructure produced by laser cladding is shown on Fig. 2. The microstructure of the overlap cladding was periodic in characteristic. The morphologies of the microstructure were mainly affected by the degree of the constitutional supercooling and the cooling rate. Nevertheless, on deposition of successive cladding layers, phase transformations were induced on the previous cladding material, mainly by the thermal effect of the laser heat input.[10,16,17]

In the single track of laser cladding, the cellular grains grew perpendicularly to the interface, the direction of the greatest temperature gradient. The equiaxed grains are situated in theenter of the layer because of violent perturbation of the melten pool. Similar equiaxed grains occurred on the top layer of the multicladding layers.

The microstructures of the multicladding layers are composed of equiaxed grains, cellular grains with martensite structure, and coarse grains with tempered martensite structure. The equiaxed grains were located in the center of every track, and the cellular grains surrounded the equiaxed grains, whereas the coarse grains were situated in the zones between successive claddings. The cellular grains are on the side of the last cladding, and the coarsened grains are on the side of the previous claddings. The microstructures of the multicladding layers from the

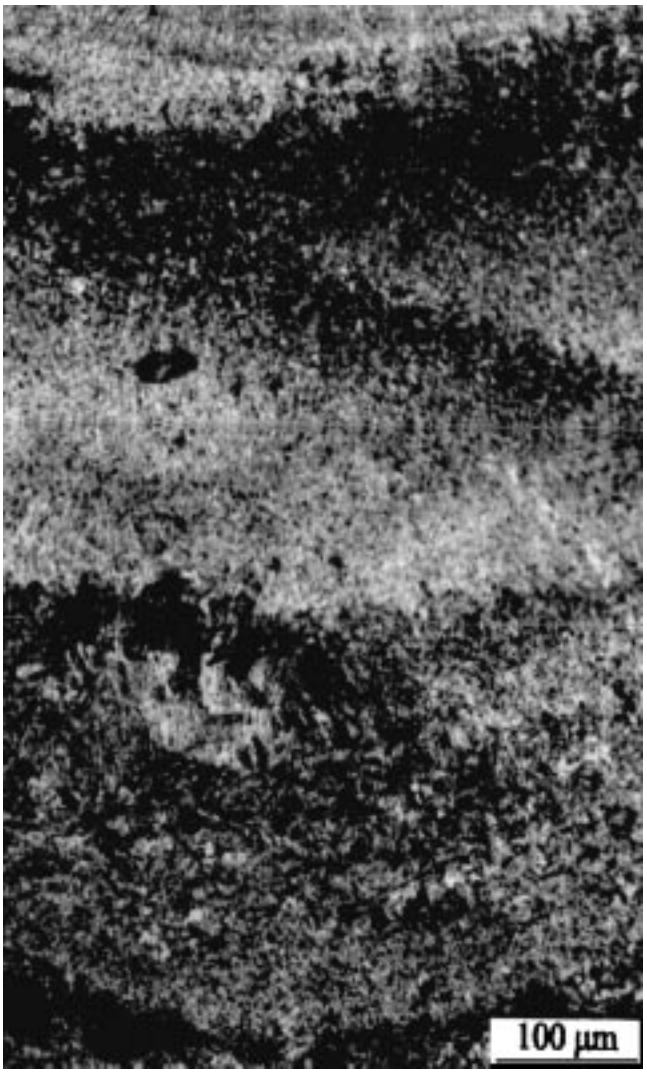

Fig. 3 The microstructure of the multicladding layer

bottom to the upper layers are shown on Fig. 3. It was recognized that the upper layer had a finer microstructure than the layers below. The microstructure of the top layer was just like that of single cladding, whereas those of the layers below, which experienced phase transformation, were different. The bottom layers were coarse grains of tempered martensite.

Because of tempering at 600 °C to avoid cracking after cladding, tempered martensite appeared in the microstructure of the SAW cladding layer, which was shown on Fig. 4. The structure was coarser than that of laser cladding, because SAW cladding introduced higher heat input.

3.2 Hardness and Composition Distributions Analysis

The hardness distribution of a single-track laser cladding from top to bottom is shown on Fig. 5. The hardness of the cladding layer, almost uniformly distributed, was much higher than that of the substrate. The chromium content 7.8 wt.% of single-track laser cladding was measured by EDX.

The microhardness of the multicladding layer produced by

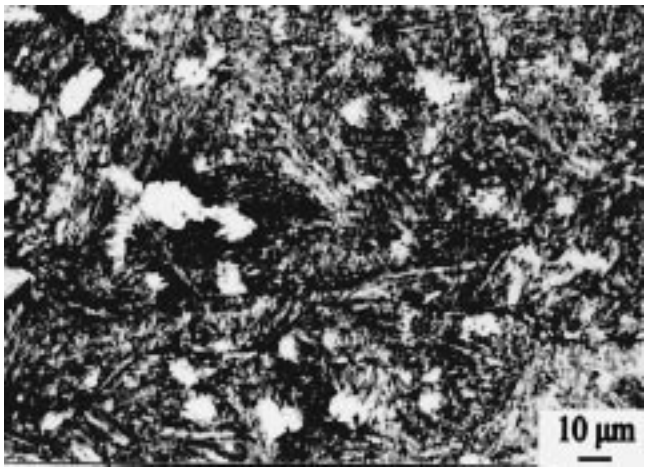

Fig. 4 The microstructure of the SAW layer with tempered martensite

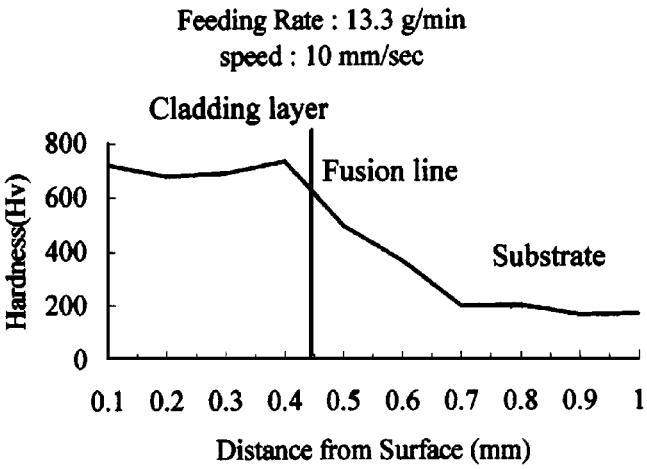

Fig. 5 The hardness distributions of single track laser cladding

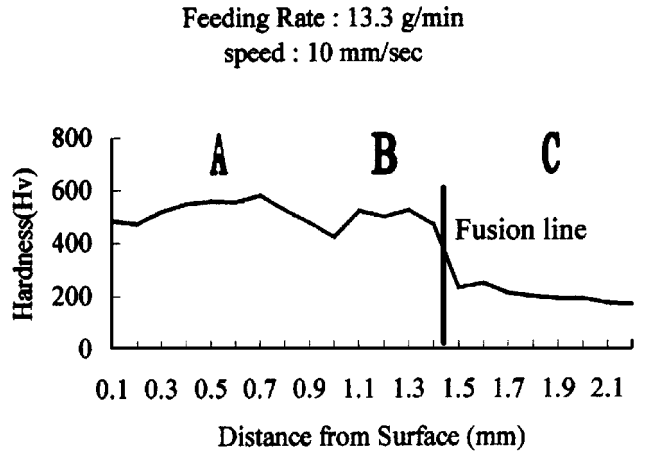

Fig. 6 The hardness distribution measured on line 1

laser cladding was measured in two directions, longitude (line 1, ABC) and latitude (line 2, DEF), as shown in Fig. 2. Figure 6 illustrates the hardness distribution along line 1 and Fig. 7,

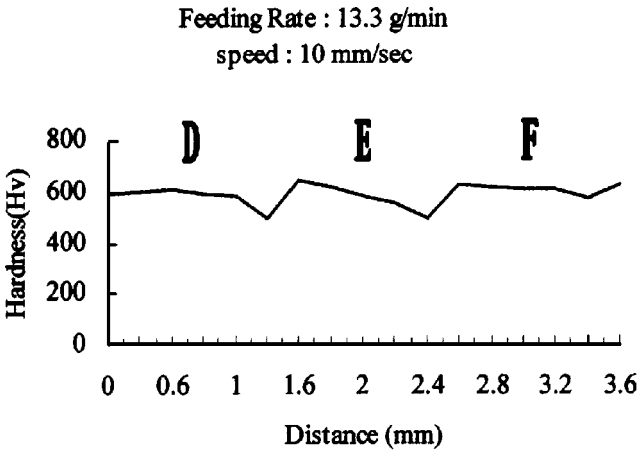

Fig. 7 The hardness distribution measured on line 2

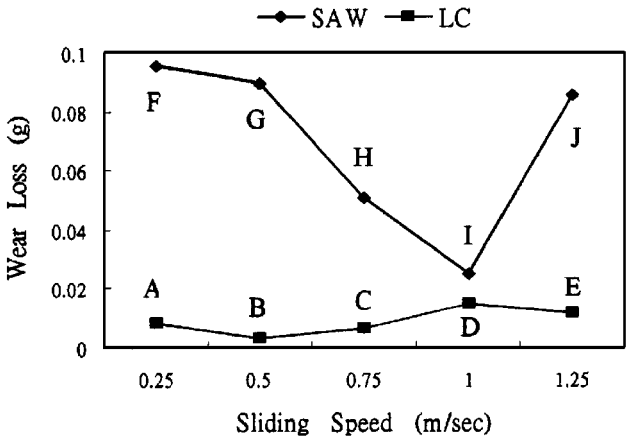

Fig. 8 The relationship between sliding speed and weight loss for the specimens A to E of laser cladding and the specimens F to J of SAW

Table 3 Chemical compositions (wt.%) of S42000 stainless steel laser cladding layer measured by GD-OES

C	Si	Mn	P	S	Cr
0.18	0.48	1.22	0.01	…	12.53

along line 2. The results show that the hardness varies with the microstructure, as indicated in Fig. 2. The softer zones between successive cladding are the tempered regions. The hardness of the substrate near the fusion line is higher than that of multicladding because of the high cooling rate, and no postheat treatment of single-track cladding induced fine microstructures and, in turn, attained higher hardness. Meanwhile, the chromium distribution measured by EPMA line scan and element mapping showed that Cr in the laser cladding layer was quite uniform with low dilution. The chromium content was also measured using EPMA and GD-OES. The result of EPMA showed that the Cr content in the laser cladding layer was 13.66 wt.%. Table 3 shows the elements measured by GD-OES. Both methods demonstrate that the amount of Cr is higher than 12 wt.%. The results indicate that the dilution in laser cladding is negligible.

3.3 Wear Analysis

The wear tests of the claddings produced by both methods were carried out with different sliding speeds. Figure 8 shows the relationship between sliding speeds and weight losses for the specimens A to E of laser cladding and the specimens F to J of SAW. The wear losses of specimens A to E produced by laser cladding were low and uniform irrespective of sliding speed, while for softer specimens F to J, the wear losses first decreased and then increased as the sliding speed increased. Less weight loss of laser cladding than that of SAW cladding is shown. Presumably, the level of hardness is responsible for the observed discrepancy in wear loss: the microhardness of SAW cladding is about Hv 372, which is consistent with Ref.10, much less than that of laser cladding (Hv600).

4. Conclusions

- The microstructures of laser cladding consist of equiaxed grain, cellular grain, and coarsened grain with tempered microstructure.
- The chromium distributions of the laser cladding layer are quite uniform. The dilution of multicladding layers by laser cladding is low under a powder feed rate of 13.3 g/min. The chromium content remains greater than 12 wt.%.
- The wear resistance of laser cladding is superior to that of SAW cladding at all sliding speeds except at 1 m/s, at which both show similar wear loss.

Acknowledgments

Financial support from the National Science Council of the Republic of China under Grant No. NSC87-2216-E-011-030 is gratefully acknowledged.

References

1. M. Crowther: *Met. Constr.*, 1984, May, pp. 277-81.
2. S. Merrick: *Welding J.*, 1994, Apr., pp. 53-56.
3. D.J. Kotecki: *Welding J.*, 1994, Jan., pp. 16-23.
4. H.L. Tsai, Y.S. Tarng, and C.M. Tseng: *Int. J. Adv. Manuf. Technol.*, 1996, vol.12, pp. 402-06.
5. B. Irving: *Welding J.*, 1991, Aug., pp. 37-40.
6. E. Ramous: in *High Power Laser*, A. Niku-Lari and B.L. Mordike, eds., Pergamon Press, New York, NY, 1989, pp. 13-25.
7. G.B. Viswanathan and R. Sivakumar: *Key Eng. Mater.*, 1989, vol. 38, pp. 393-412.
8. Y. Yoshida and T. Hirozane: *Welding Int.*, 1989, No. 9, pp. 799-804.
9. B.C. Oberlander and E. Lugscheider: *Mater. Sci. Technol.*, 1992, vol. 8 (8), pp. 657-65.
10. M. Riabkina-Fishman and J. Zahavi: in *High Power Laser*, A. Niku-Lari and B.L. Mordike, eds., Pergamon Press, New York, NY, 1989, pp. 101-15.
11. B.L. Mordike and W.N. Kahrmann: in *High Power Laser*, A. Niku-Lari and B.L. Mordike, eds., Pergamon Press, New York, NY, 1989, pp. 41-47.
12. H. de Beurs and J.T.M. de Hosson: in *High Power Laser*, A. Niku-

Lari and B.L. Mordike, eds., Pergamon Press, New York, NY, 1989, pp. 27-38.
13. M. Takemoto: in *High Power Laser*, A. Niku-Lari and B.L. Mordike, eds., Pergamon Press, New York, NY, 1989, pp. 75-88.
14. P.Z. Wang, Y.S. Yang, G. Ding, J.X. Qu, and H.S. Shao: *Wear*, 1997, vol. 209, pp. 96-100.
15. J.Y. Jeng, B.E. Quayle, P.J. Modern, W.M. Steen, and D.B. Bastow: *Corr. Sci.*, 1993, vol. 35, pp. 1289-96.
16. G. Shi, J. Liu, P. Ding, and S. Zhou: *Mater. Sci. Technol.*, 1998, vol. 14, pp. 80-84.
17. A. Houndri, S. Polymenis, Y. Chryssoulakis, and D. Pantelis: *Metall. Trans. A*, 1992, vol. 23A, pp. 1801-06.
18. M. Bamberger, W.D. Kaplan, B. Medres, and L. Shepeleva: *J. Laser Appl.*, 1998, vol. 10 (1), pp. 29-33.
19. E.M. Breinan and B.H. Kear: in *Laser Materials Processing*, M. Bass, ed., North-Holland Publishing Company, Amsterdam, 1983, pp. 237-95.
20. J.A. Brooks and K.W. Mahin: in *Welding: Theory and Practice*, D.L. Olson, R. Dixon, and A.L. Liby, eds., Elsevier Science Publishers B.V., Amsterdam, 1990, pp. 37-78.